Dalton Transactions

ROYAL SOCIETY OF CHEMISTRY

FRONTIER

View Article Online
View Journal | View Issue

Cite this: *Dalton Trans.*, 2024, **53**, 18083

Recent advances in polyoxometalate-based catalysts for light-driven hydrogen evolution

Mengyun Zhao, Qingqing Liu, Yeqin Feng and Hongjin Lv *

Received 18th August 2024,
Accepted 27th September 2024

DOI: 10.1039/d4dt02357a

rsc.li/dalton

The photocatalytic hydrogen evolution reaction has been considered as an efficient route to addressing energy and environmental issues. As an interesting class of multi-electron transfer catalysts, polyoxometalates (POMs) have been widely used for photocatalytic hydrogen evolution due to their tunable geometrical and electronic structures, reversible electron storage capacity, and preeminent redox properties. This Frontier article highlights our recent advances in the construction of efficient POM-based photocatalytic hydrogen evolution systems in terms of three aspects, including polyoxometalate-based catalysts, light-absorbing photosensitizers, and sacrificial reagents.

Introduction

Considering the severe energy shortage and environmental pollution facing modern society, the exploration of clean, environmentally friendly, and renewable energy alternatives has become an urgent issue.[1–3] Solar energy has received researchers' attention because of its abundant reserves and renewable, clean and other characteristics; however, because of the intermittent, random, and regional existence of solar energy, the direct application of solar energy is not convenient.[2,4,5] Using photocatalytic reactions to store intermittent solar energy in chemical bonds is a promising approach, with solar-driven hydrogen evolution receiving much attention from researchers.[2,3] To achieve high photocatalytic efficiency, many representative photocatalysts have been developed, including noble metal complexes, organic dyes, metal oxides/sulfides/nitrides/hydroxides, *etc.*[2,6–8] However, developing novel photocatalysts to enhance solar energy utilization efficiency in the photocatalytic hydrogen evolution process has substantial and promising implications.

Polyoxometalates (POMs), with rich redox chemistry, adjustable electronic and geometric properties, and reversible electron-storage capabilities, have attracted considerable research interest from researchers working in the photocatalytic hydrogen production area.[9–11] Polyoxometalates are a class of metal–oxygen clusters formed by condensation of oxygen-containing acid radicals of W, Mo, V, Nb, and Ta transition metal ions. The basic building blocks of POMs are mainly $\{MO_6\}$ octahedra and $\{XO_4\}$ (X = Si, Ge, P, *etc.*) tetrahedra, with a wide variety of structures formed between polyhedra through co-angles, co-edges, or co-planes.[2,9–12] Because of the continuous development of single-crystal diffractometers, POM chemistry has also been rapidly developed, and there are six classical structures of POMs: Keggin, Wells-Dawson, Silverton, Waugh, Anderson, and Lindqvist (Fig. 1).[10] The most studied of these are Keggin ($[XM_{12}O_{40}]^{m-}$, X = P, Si, Ge, As, *etc.*; M = W and Mo) and Wells-Dawson ($[X_2M_{18}O_{62}]^{n-}$, X = P and As; M = W and Mo). When the saturated Keggin and Wells-Dawson structures lose one or more $\{MO_6\}$ octahedra, the O coordination sites can be released, and the O-ligand sites from the lacunary POMs can bind other transition metals to form transition-metal-substituted POMs (TMSPOMs).[2,13] Introducing transition metal ions not only enriches the structure of POMs but also endows them with richer physicochemical properties. Various synthetic strategies have been developed to design the

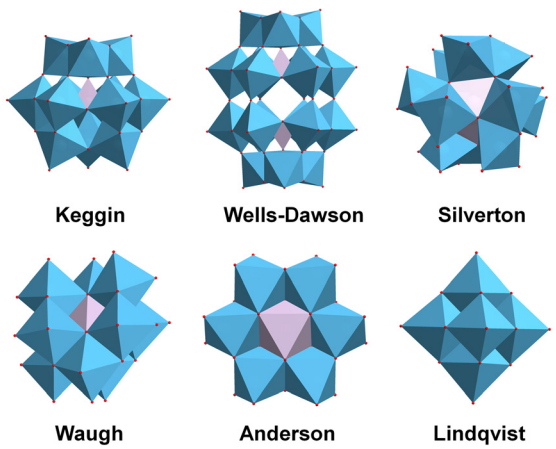

Fig. 1 Six classical polyoxometalate structures.

MOE Key Laboratory of Cluster Science, Beijing Key Laboratory of Photoelectric/Electrophotonic Conversion Materials, School of Chemistry and Chemical Engineering, Beijing Institute of Technology, Beijing 102488, China.
E-mail: hlv@bit.edu.cn

structures of POMs at the atomic level, realizing the adjustment of their composition, electronic structure and counterions based on different reaction types.

The unique characteristics of POMs make them widely used in catalytic reactions.[9] The use of POMs in light-driven hydrogen evolution has a long history, with nearly half a century of development since 1985.[14] In 2021, our group presented an exhaustive summary of POM-based photocatalytic hydrogen evolution systems, in which the authors classified the catalytic systems into two main categories according to the light source used: (1) UV/near-UV and (2) visible light.[2] When UV/near-UV light is used as a light source, POMs act as light absorbers and catalysts in the photocatalytic hydrogen evolution system. Under UV/near-UV irradiation, intramolecular oxygen-to-metal charge transfer ($O_{2p} \rightarrow W_{5d}$) occurs in POMs, in which electrons from the spin-paired highest occupied molecular orbitals (HOMOs) will be excited to the lowest unoccupied molecular orbitals (LUMOs) and delocalized.[15] Sacrificial electron donors (sacrificial reagents) are oxidized in the O_{2p} orbitals, ultimately enabling the formation of reduced-state POMs (heteropoly blue). POMs or reduced-state POMs have a high negative charge and can store multiple protons. Reduced-state POMs can catalyze the reduction of protons to produce hydrogen, and the process can be accelerated by the presence of noble metals (Scheme 1).[2] Heteropolyoxometalates, isopolyoxometalates, and TMSPOMs have been successively used for UV-driven hydrogen evolution from water decomposition. Given that ultraviolet (UV) and near-UV light account for only a minor fraction of the solar spectrum, the development of visible-light-driven hydrogen production systems has attracted considerable interest over the years.

When visible light is used as the light source, POMs mainly act as catalysts with a multi-electron transfer body, and the system requires an additional photosensitizer to enhance light absorption. After years of development, in 2014, Hill's group developed a three-component photocatalytic water-splitting hydrogen evolution system, which includes a light-absorbing photosensitizer, a multi-electron transfer POM catalyst, and an easily oxidized sacrificial reagent.[16] From 2020 to the present, researchers have been committed to researching hydrogen evolution systems of POM-based catalysts driven by visible light, and catalysts, photosensitizers, and sacrificial reagents have been explored and optimized. Here, we briefly review our recent research progress of POM-based photocatalytic hydrogen evolution systems and prospect the development of this field.

Novel POMs as catalysts

Benefiting from advanced synthetic strategies and sufficient characterization techniques, POMs can be designed and regulated with atomic-level precision, making it easier to study the relationships between the structure and properties. As for TMSPOMs, the existence of abundant transition metal active sites could be beneficial for improving the photocatalytic hydrogen evolution activity.[13] Based on this, several novel TMSPOMs were synthesized and successfully used to construct a three-component system for photocatalytic hydrogen evolution research.[17–38]

In 2024, our group successfully synthesized a tetrahedral POM-based organic cage (POC) $K_3Na_{17}H_{12}[(C_4H_6O_6)_6[Ni_4(OH)_3(A\text{-}\alpha\text{-}SiW_9O_{34})]_4]\cdot 96H_2O$ ($Ni_{16}L_6(SiW_9)_4$) (Fig. 2).[36] The $Ni_{16}L_6(SiW_9)_4$ tetrahedron is constructed using six flexible L-(+)-tartaric acid ligands and four Ni_4-substituted Keggin clusters (Ni_4SiW_9), forming a cage-like structure with a void space of about 102 Å^3. The photocatalytic activity of the catalyst TBA–$Ni_{16}L_6(SiW_9)_4$ was analyzed under visible light irradiation using TEOA as a sacrificial donor and $[Ir(coumarin)_2(dtbbpy)]^+$ as a photosensitizer. Under minimally optimized conditions, the hydrogen evolution system achieves a TON of 6834 after 5 h of reaction. Furthermore, by extending the reaction time to 96 hours, the TON value progressively increases to 15 500. Owing to the distinctive cage-like configuration of $Ni_{16}L_6(SiW_9)_4$ POCs, the TBA–$Ni_{16}L_6(SiW_9)_4$ catalytic reaction system possesses greater accessibility of catalyst components in contrast to the non-cage TBA–$Ni_{16}(PO_4)_4(PW_9)_4$ catalytic system. This work diversifies the family of organic cages based on POMs and extends the novel catalytic application of POCs in solar-driven hydrogen evolution.

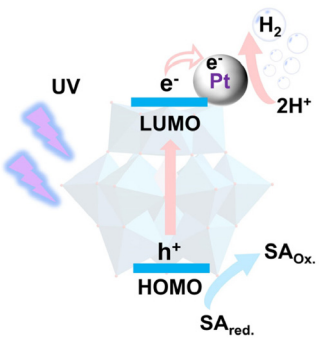

Scheme 1 Schematic of photocatalytic H_2 evolution using a POM-based photocatalyst under UV-light irradiation.

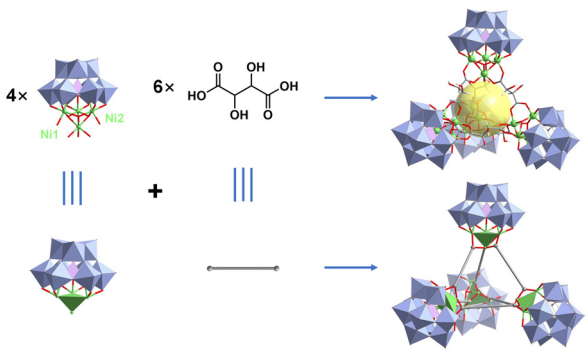

Fig. 2 Polyhedral and ball-and-stick representation of the structure of $Ni_{16}L_6(SiW_9)_4$. Reprinted with permission from ref. 36. Copyright 2023 Elsevier.

Inspired by the principle of molecular orbital engineering, very recently, we successfully synthesized and characterized two well-defined POMs, $[H_2N(CH_3)_2]_{9.24}Na_3H_4[Cu_{2.06}W_{1.94}O_2(P_2W_{16}O_{60})_2]\cdot 40H_2O$ (POM-1) and $[H_2N(CH_3)_2]_{12.6}Na_2H_3[Cu_{2.4}Mo_{6.48}W_{3.12}O_{26}(P_2W_{12}O_{48})_2]\cdot 27H_2O$ (POM-2), and the two POMs exhibited analogous twin-Dawson-type polyoxoanion skeletons (Fig. 3).[37] The photocatalytic system, which incorporates POM-1/POM-2, the photosensitizer $[Ir(coumarin)_2(dtbbpy)]^+$, and the electron donor TEOA, was employed for the generation of hydrogen under Xe lamp irradiation. These two POM compounds demonstrated remarkable photocatalytic activity, with TONs of 2277 and 4722.5, respectively. The catalytic performance is closely related to the lowest unoccupied molecular orbital (LUMO) level of POMs, and the incorporation of molybdenum (Mo) addenda atoms into POM-2 can effectively modulate its LUMO level, resulting in a stronger driving force for the thermodynamically favorable and efficient transfer of electrons from the photosensitizer to POM-2. This higher driving force could significantly contribute to more efficient photocatalytic hydrogen evolution activity under visible light irradiation.

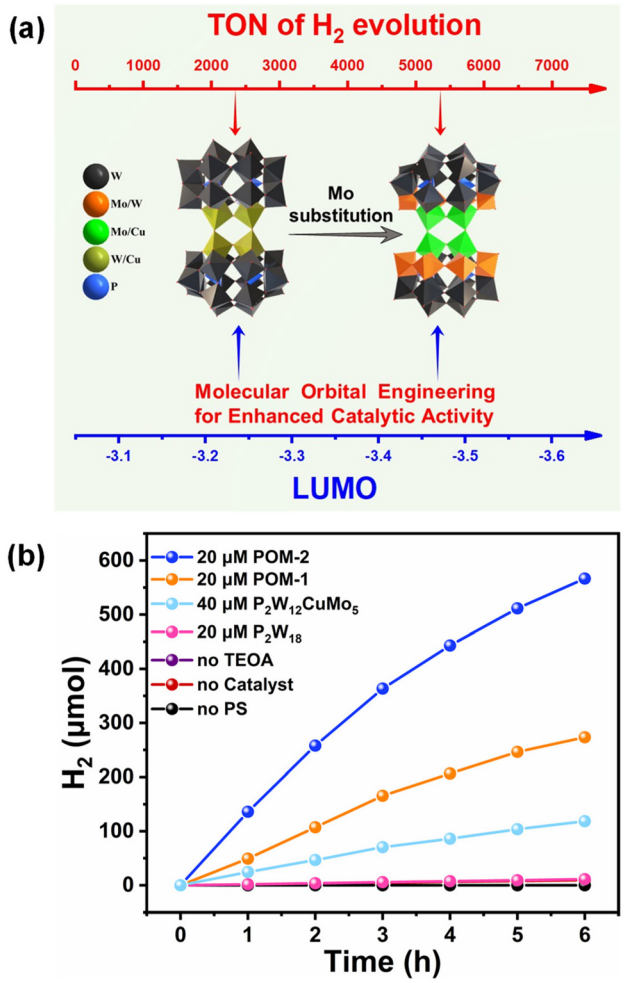

Fig. 3 (a) X-ray crystal structures and the LUMO of POM-1 and POM-2. (b) Visible light-driven hydrogen evolution kinetics of different control experiments. Adapted with permission from ref. 37. Copyright 2024 American Chemical Society.

Photosensitizers

In these above-reported studies, the catalytic mechanism of reaction systems using an Ir complex as the photosensitizer could be proposed as shown in Scheme 2.[39]

For soluble noble-metal complexes and organic molecular photosensitizers, recyclable and separated semiconductor MOFs with absorbent units have been used as photosensitizers. The strong host–guest interaction between POMs and MOFs results in better photocatalytic performance, durability and reusability of POM@MOF composites.[40–43] With this in mind, our group prepared two tri-nickel-containing POM@MOF composites, $Ni_3P_2W_{16}$@NU-1000 ($Ni_3P_2W_{16}$ = $Na_4Li_5[Ni_3(OH)_3(H_2O)_3P_2W_{16}O_{59}]$) and Ni_3PW_{10}@NU-1000 (Ni_3PW_{10} = $K_6Na[Ni_3(H_2O)_3PW_{10}O_{39}H_2O]$), through strong host–guest interaction using a simple and broad-spectrum impregnation method (Fig. 4).[42] Combined with ascorbic acid (AA) as the sacrificial electron donor, a three-component photocatalytic hydrogen production system was constructed. Under optimized conditions, the resulting POM@MOF composite demonstrated efficient photocatalytic hydrogen generation from a water-compatible system. Notably, such a composite catalyst can not only operate in the absence of precious metals as co-catalysts, but also exhibit superior long-term stability and reusability. The hydrogen evolution rates of $Ni_3P_2W_{16}$@NU-1000 and Ni_3PW_{10}@NU-1000 are 13 051 and 3482 μmol g^{-1} h^{-1}, respectively. Significantly, such a POM@NU-1000 composite catalyst also exhibited decent hydrogen evolution activity under natural sunlight irradiation,

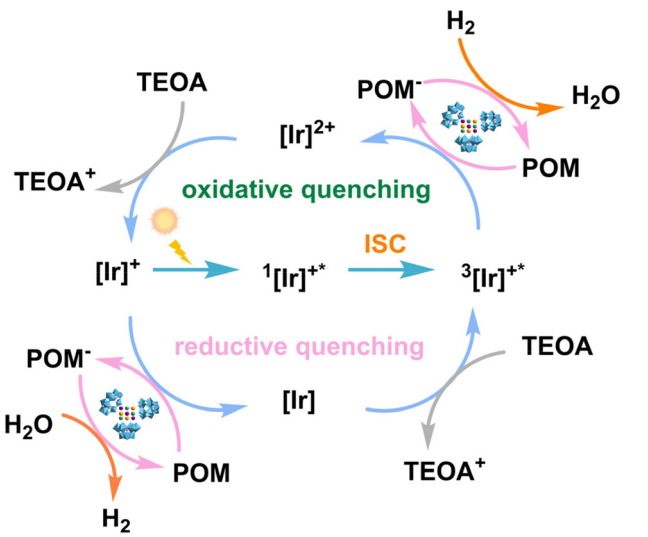

Scheme 2 Schematic of photocatalytic H_2 evolution using a POM photocatalyst and an Ir complex photosensitizer under visible-light irradiation.

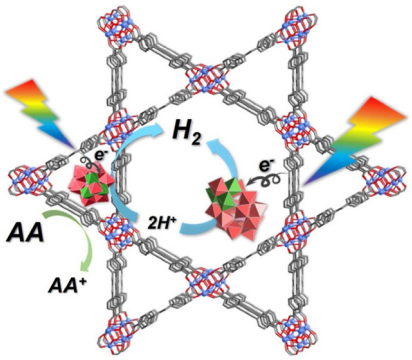

Fig. 4 Structural model of $Ni_3P_2W_{16}$@NU-1000 and the schematic diagram of photocatalytic hydrogen production. Reprinted with permission from ref. 42. Copyright 2021 Elsevier.

demonstrating the potential of this photocatalytic system in large-scale production.

Compared with noble metal-based organometallic chromophores and highly luminescent organic dyes, semiconductors (CdSe/S, ZnInS, TiO_2, C_3N_4, *etc.*) exhibit excellent advantages, such as outstanding light stability, adjustable redox potential, size-dependent absorption characteristics and large absorption cross sections of the entire visible spectrum, and have been used in photocatalytic hydrogen evolution systems.[44–50] In 2022, we developed an aqueous-phase-stable and durable hydrogen production system by integrating a water-soluble CdSe quantum dot (QD) photosensitizer with an electron donor (AA) and diverse core Ni-substituted polyoxometalates (POMs) including Ni_3P ($K_6Na[Ni_3(H_2O)_3PW_{10}O_{39}H_2O]\cdot12H_2O$), Ni_4P_2 ($Na_6K_4[Ni_4(H_2O)_2(PW_9O_{34})_2]\cdot32H_2O$), Ni_9P_3 ($K_5Na_{11}[Ni_9(OH)_3(H_2O)_6(HPO_4)_2(PW_9O_{34})_3]\cdot55H_2O$), and $Ni_{16}P_4$ ($Na_{18}K_{10}[\{Ni_4(OH)_3PO_4\}_4(A\text{-}\alpha\text{-}PW_9O_{34})_4]\cdot75H_2O$) as catalysts (Fig. 5).[46] Under visible light irradiation, the CdSe + POM catalytic system has demonstrated superior hydrogen production capabilities, outperforming other semiconductor/POM hybrid systems for photocatalytic hydrogen generation. The photocatalytic system catalyzed by Ni_4P_2 achieved a TON of 9000 after 12 h, equating to a hydrogen production rate of 138 mmol g^{-1} h^{-1}. This performance is notably superior to that of catalytic systems incorporating organometallic chromophores. Furthermore, the activities of POM catalysts with different Ni centers were compared, and the catalytic hydrogen production activity is positively correlated with the nuclearity degree of the Ni center in the POM catalyst. Various experiments and spectral analyses show that the synergistic effect of the CdSe photo-absorbent, Ni-substituted POM catalyst with excellent reversible multi-electron transfer and AA electron donor with fast hole removal is the reason for the excellent performance of this catalytic system.

Sacrificial reagents

In the above three-component system, the sacrificial reagents are mostly simple organic molecules (TEOA, TEA, AA, *etc.*), which are oxidized to products with low economic value after photocatalysis. Hence, the oxidation end of the photocatalyzed water decomposition half-reaction is not fully utilized. Therefore, researchers use organic substrates as sacrificial reagents that can be transformed into high-value chemicals and carry out coupling hydrogen production to use the oxidation and reduction ends fully.[48,50,51]

In 2024, we successfully developed an efficient photocatalytic system by integrating cadmium sulfide nanorods (CdS NRs) with Ni_4P_2, achieving high selectivity in the photooxidative dehydrogenative coupling of 4-methoxythiophenol (4-MTP) to produce 4-methoxydiphenyl disulfide (4-MPD) and hydrogen with a high yield (Fig. 6).[51] Under optimized conditions, this system achieved a conversion rate of 4-MTP up to 98.39%, a selectivity for 4-MPD of 94.99%, and a hydrogen yield of 25.96 μmol. The catalytic system exhibits high catalytic activity for 4-MTP and good universality for other thiophenol compounds. The Ni_4P_2/CdS composite system has shown excellent stability throughout the photocatalytic cycles. Reaction mechanism analysis indicates that CdS NRs generate photogenerated electron–hole pairs under visible light excitation. The photogenerated holes directly participate in the

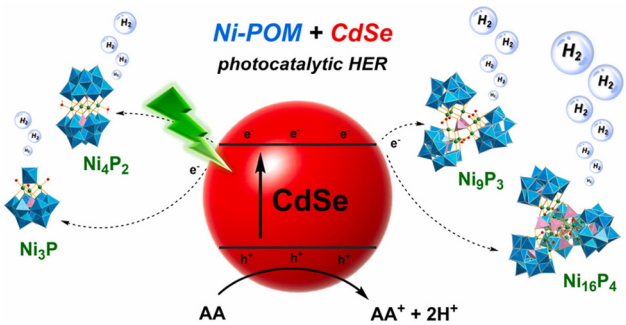

Fig. 5 Proposed schematic mechanism of catalytic reactions using Ni-substituted POMs and CdSe QDs. Reprinted with permission from ref. 46. Copyright 2022 Elsevier.

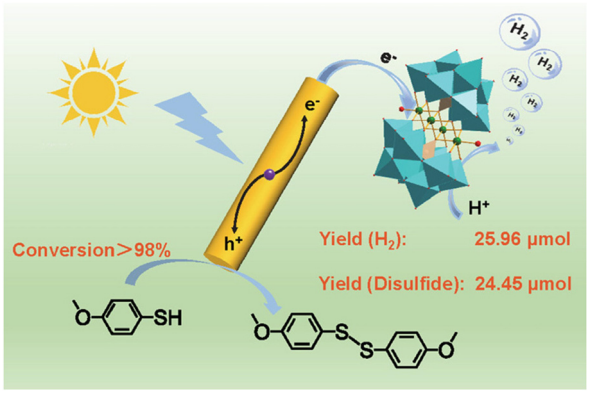

Fig. 6 Proposed schematic mechanism of catalytic reactions using Ni_4P_2, CdS NRs, and 4-MTP. Reprinted with permission from ref. 51. Copyright 2024 Elsevier.

oxidation of the S–H bond in 4-MTP, producing $SC_6H_4(OCH_3)$ intermediates and active hydrogen species, which undergo a radical coupling reaction to form the target product 4-MPD. Concurrently, the photogenerated electrons are transferred to the Ni_4P_2 catalyst, where the nickel center captures and activates these hydrogen species, promoting hydrogen gas generation. The synergistic effect between CdS NRs and Ni_4P_2 significantly enhances the separation efficiency of photogenerated charges, thereby enhancing the dehydrogenative coupling performance of the entire photocatalytic system. This research outcome provides a novel strategy for photocatalytic synthesis and opens new possibilities for solar energy-driven chemical transformations, holding significant scientific importance and application prospects.

Conclusions and outlook

Polyoxometalates have been extensively utilized in photocatalytic hydrogen evolution due to their abundant and diverse structures, adjustable composition and electronic configuration, reversible electronic storage capability, and outstanding redox properties. We have briefly highlighted our recent progress in rationally constructing a more promising photocatalytic hydrogen production system from the aspects of POM catalysts, photosensitizers, and sacrificial reagents. In such existing three-component photocatalytic systems, all three components are indispensable, and many aspects of research can be further advanced in the future.

For catalysts, the catalytic performance is closely related to the number of active sites, the degree of energy level matching, and the mass transfer rate of the catalytic system. Therefore, it is essential to synthesize TMSPOMs with novel structures and energy level matching. This can be achieved through the following approaches: (i) synthesizing POCs with a molecular cage structure to facilitate mass transfer and (ii) increasing the driving force of electron transfer by adjusting molecular orbitals to match photosensitizers and achieve improved catalytic activity.

In terms of photosensitizers, it is very important to develop photosensitizers with a broad light-absorption range and strong absorbing ability by introducing a wide absorption range chromophore into organometallic complexes, so that the light utilization efficiency can be improved. In addition, exploring more relatively inexpensive semiconductors as photosensitizers will help reduce the cost of photocatalytic hydrogen production.

For sacrificial reagents, the sacrificial electron donor can be replaced with organic substrates with value-added potential to promote the hydrogen production of POM-based photocatalytic systems and the conversion of organic substrates, such as organic oxidation reactions, oxidative coupling reactions (C–C, C–N, and S–S coupling reactions), and photoreforming reactions using organic plastics, pollutants, and biomass as the substrates.[52]

In addition, the stability and durability of the photocatalytic system over a long time are important factors to be considered. For a typical three-component photocatalytic hydrogen system, long-term stable operation needs to meet some criteria, including: (1) a sufficient concentration of the sacrificial reagent to replenish the oxidation end and (2) the stability of the structures of POMs and photosensitizers during the reaction. As the reaction proceeds over a long time, the sacrificial reagent will be consumed. When the concentration is insufficient, the catalytic performance may degrade over time. This problem can be solved by replenishing the sacrificial reagent in time. POMs and photosensitizers may also be intolerant during long-term reactions, leading to a degraded catalytic performance. Therefore, the development of POMs and photocatalysts with more stable structures is also a very promising research direction in the future.

Finally, we hope this review will provide some valuable guidelines for developing more efficient and robust POM-based photocatalytic hydrogen production systems and the related interdisciplinary research areas.

Data availability

No primary research results, software or code have been included and no new data were generated or analysed as part of this review.

Conflicts of interest

There are no conflicts to declare.

Acknowledgements

This work was supported by the Natural Science Foundation of Beijing Municipality (2242017), the National Natural Science Foundation of China (21871025), the Recruitment Program of Global Experts (Young Talents), and the BIT Excellent Young Scholars Research Fund. The support from the Analysis and Testing Center of Beijing Institute of Technology is also highly appreciated.

References

1 Z. Wang, C. Li and K. Domen, *Chem. Soc. Rev.*, 2019, **48**, 2109–2125.
2 M. Zhang, H. Li, J. Zhang, H. Lv and G.-Y. Yang, *Chin. J. Catal.*, 2021, **42**, 855–871.
3 N. Pirrone, F. Bella and S. Hernández, *Green Chem.*, 2022, **24**, 5379–5402.
4 T.-Z. Ang, M. Salem, M. Kamarol, H. S. Das, M. A. Nazari and N. Prabaharan, *Energy Strategy Rev.*, 2022, **43**, 100939–100965.
5 H. H. Pourasl, R. V. Barenji and V. M. Khojastehnezhad, *Energy Rep.*, 2023, **10**, 3474–3493.

6 J. Huo, Y.-B. Zhang, W.-Y. Zou, X. Hu, Q. Deng and D. Chen, *Catal. Sci. Technol.*, 2019, **9**, 2716–2727.
7 M. Shao, Y. Shao and H. Pan, *Phys. Chem. Chem. Phys.*, 2024, **26**, 11243–11262.
8 Y. Wang, Z. Ding, N. Arif, W.-C. Jiang and Y.-J. Zeng, *Mater. Adv.*, 2022, **3**, 3389–3417.
9 S.-S. Wang and G.-Y. Yang, *Chem. Rev.*, 2015, **115**, 4893–4962.
10 D.-L. Long, E. Burkholder and L. Cronin, *Chem. Soc. Rev.*, 2007, **36**, 105–121.
11 H. Lv, Y. V. Geletii, C. Zhao, J. W. Vickers, G. Zhu, Z. Luo, J. Song, T. Lian, D. G. Musaev and C. L. Hill, *Chem. Soc. Rev.*, 2012, **41**, 7572–7589.
12 C. L. Hill, *Chem. Rev.*, 1998, **98**, 1–2.
13 A. Patel, N. Narkhede, S. Singh and S. Pathan, *Catal. Rev.*, 2016, **58**, 337–370.
14 C. L. Hill and D. A. Bouchard, *J. Am. Chem. Soc.*, 1985, **107**, 5148–5157.
15 R. Ian Buckley and R. J. H. Clark, *Coord. Chem. Rev.*, 1985, **65**, 167–218.
16 H. Lv, W. Guo, K. Wu, Z. Chen, J. Bacsa, D. G. Musaev, Y. V. Geletii, S. M. Lauinger, T. Lian and C. L. Hill, *J. Am. Chem. Soc.*, 2014, **136**, 14015–14018.
17 H. Li, L. Qin, L.-Y. Yao and H. Lv, *J. Coord. Chem.*, 2020, **73**, 2410–2421.
18 T. Cui, L. Qin, F. Fu, X. Xin, H. Li, X. Fang and H. Lv, *Inorg. Chem.*, 2021, **60**, 4124–4132.
19 J.-J. Sun, W.-D. Wang, X.-Y. Li, B.-F. Yang and G.-Y. Yang, *Inorg. Chem.*, 2021, **60**, 10459–10467.
20 H.-L. Li, M. Zhang, C. Lian, Z.-L. Lang, H. Lv and G.-Y. Yang, *CCS Chem.*, 2021, **3**, 2095–2103.
21 Y. Smortsova, C. Falaise, A. Fatima, M. Ha-Thi, R. Méallet-Renault, K. Steenkeste, S. Al-Bacha, T. Chaib, L. Assaud, M. Lepeltier, M. Haouas, N. Leclerc, T. Pino and E. Cadot, *Chem. – Eur. J.*, 2021, **27**, 17094–17103.
22 E. Tanuhadi, J. Cano, S. Batool, A. Cherevan, D. Eder and A. Rompel, *J. Mater. Chem. C*, 2022, **10**, 17048–17052.
23 S.-S. Wang, X.-Y. Kong, W. Wu, X.-Y. Wu, S. Cai and C.-Z. Lu, *Inorg. Chem. Front.*, 2022, **9**, 4350–4358.
24 Y. Feng, L. Qin, J. Zhang, F. Fu, H. Li, H. Xiang and H. Lv, *Chin. J. Catal.*, 2022, **43**, 442–450.
25 Z.-W. Wang, Q. Zhao, C.-A. Chen, J.-J. Sun, H. Lv and G.-Y. Yang, *Inorg. Chem.*, 2022, **61**, 7477–7483.
26 M. Chi, H. Li, X. Xin, L. Qin, H. Lv and G.-Y. Yang, *Inorg. Chem.*, 2022, **61**, 8467–8476.
27 Y.-H. Zhu, Z.-Y. Du, J.-L. Wang, J.-B. Yang, H. Mei and Y. Xu, *Inorg. Chem.*, 2022, **61**, 20397–20404.
28 Q. Zhao, X. Li, Y. Wang, H. Lv and G. Yang, *Nanomaterials*, 2023, **13**, 2009–2020.
29 Z.-W. Wang and G.-Y. Yang, *Molecules*, 2023, **28**, 664–672.
30 Y. Wang, X. Xin, Y. Feng, M. Chi, R. Wang, T. Liu and H. Lv, *Molecules*, 2023, **28**, 2017–2030.
31 Z. Wang, X. Xin, Z. Li, M. Zhang, J. Zhang, Y. Feng, J. Zhang, H. Lv and G.-Y. Yang, *Sci. China: Chem.*, 2023, **66**, 1771–1780.
32 J.-L. Chen, Z.-W. Wang, P.-Y. Zhang, H. Lv and G.-Y. Yang, *Inorg. Chem.*, 2023, **62**, 10291–10297.
33 W. Chen, H. Li, Y. Jin, W. Lei, Q. Bai, P. Ma, J. Wang and J. Niu, *Inorg. Chem.*, 2023, **62**, 18079–18086.
34 H. Xu, Q. Chen, J.-L. Wang, Q. Wang, C.-Y. Jiao, P.-F. Yan, H. Mei and Y. Xu, *Inorg. Chem.*, 2023, **62**, 18878–18886.
35 Z.-W. Wang, C.-A. Chen and G.-Y. Yang, *Dalton Trans.*, 2024, **53**, 9812–9818.
36 J. Li, Y. Feng, F. Fu, X. Xin, G. Yang and H. Lv, *Chin. Chem. Lett.*, 2024, **35**, 108736–108740.
37 M. Chi, Y. Zeng, Z.-L. Lang, H. Li, X. Xin, Y. Dong, F. Fu, G.-Y. Yang and H. Lv, *ACS Catal.*, 2024, **14**, 5006–5015.
38 P.-Y. Zhang, C. Lian, Z.-W. Wang, J. Chen, H. Lv and G.-Y. Yang, *Dalton Trans.*, 2024, **53**, 13409–13415.
39 L. Qin, C. Zhao, L.-Y. Yao, H. Dou, M. Zhang, J. Xie, T.-C. Weng, H. Lv and G.-Y. Yang, *CCS Chem.*, 2022, **4**, 259–271.
40 Z.-M. Zhang, T. Zhang, C. Wang, Z. Lin, L.-S. Long and W. Lin, *J. Am. Chem. Soc.*, 2015, **137**, 3197–3200.
41 L. Jiao, Y. Dong, X. Xin, R. Wang and H. Lv, *J. Mater. Chem. A*, 2021, **9**, 19725–19733.
42 L. Jiao, Y. Dong, X. Xin, L. Qin and H. Lv, *Appl. Catal., B*, 2021, **291**, 120091–120101.
43 R. Wang, Y. Feng, L. Jiao, Y. Dong, H. Zhou, T. Liu, X. Jing and H. Lv, *J. Mater. Chem. A*, 2023, **11**, 5811–5818.
44 X. Zhou, H. Yu, D. Zhao, X. Wang and S. Zheng, *Appl. Catal., B*, 2019, **248**, 423–429.
45 Y. Dong, Q. Han, Q. Hu, C. Xu, C. Dong, Y. Peng, Y. Ding and Y. Lan, *Appl. Catal., B*, 2021, **293**, 120214–120225.
46 M. Zhang, X. Xin, Y. Feng, J. Zhang, H. Lv and G.-Y. Yang, *Appl. Catal., B*, 2022, **303**, 120893–120901.
47 Y. Dong, Q. Hu, B. Li, X. Li, M. Chen, M. Zhang, Y. Feng and Y. Ding, *Appl. Catal., B*, 2022, **304**, 120998–121007.
48 F. Xing, R. Zeng, C. Cheng, Q. Liu and C. Huang, *Appl. Catal., B*, 2022, **306**, 121087–121097.
49 L. Tang, Y. Hu, H. Tang, L. Sun, H. Jiang, W. Wang, H. Su, J. Hu, L. Wang and Q. Liu, *J. Phys. Chem. Lett.*, 2022, **13**, 11778–11786.
50 L. Sun, X. Yu, L. Tang, W. Wang and Q. Liu, *Chin. J. Catal.*, 2023, **52**, 164–175.
51 M. Ren, T. Liu, Y. Dong, Z. Li, J. Yang, Z. Diao, H. Lv and G.-Y. Yang, *Chin. J. Catal.*, 2024, **61**, 312–321.
52 J.-H. Tang and Y. Sun, *Mater. Adv.*, 2020, **1**, 2155–2162.